Comparative Crystallography. 5. Crystal Structures, Electronic Properties, and Structural Pathways of Five $[Cu(phen)_2Br][Y]$ Complexes, Y = $[Br]^-\cdot H_2O$, $[ClO_4]^-$, $[NO_3]^-\cdot H_2O$, $[PF_6]^-$, and $[BPh_4]^-$

Gillian Murphy, Cathal O'Sullivan, Brian Murphy,† and Brian Hathaway*

The Chemistry Department, University College Cork, Ireland

Received April 24, 1997[⊗]

The crystal structures of $[Cu(phen)_2Br][Br]\cdot H_2O$ (**1**, phen = 1,10-phenanthroline), $[Cu(phen)_2Br][ClO_4]$ (**2**), $[Cu(phen)_2Br][NO_3]\cdot H_2O$ (**3**), $[Cu(phen)_2Br][PF_6]$ (**4**), and $[Cu(phen)_2Br][BPh_4]$ (**5**) have been determined by X-ray diffraction. Four of the complexes, **1**−**4**, have a CuN_4Br chromophore with a square based pyramidal distorted trigonal bipyramidal (SBPDTB) stereochemistry, while **5** involves an extreme trigonal bipyramidal distorted square based pyramidal (TBDSBP) stereochemistry. The geometries of the CuN_4Br chromophores in **1**−**5** are compared by scatter plot analysis with a single $[Cu(phen)_2Br][ClO_4]$ complex, **6**, of known crystal structure involving a crystallographic 2-fold axis of symmetry. The distortion isomers of **2** and **6** are significantly different. The scatter plots of the six cation distortion isomers of the $[Cu(phen)_2Br][Y]$ series of complexes suggest that all six complexes lie on a common structural pathway, involving a mixture of the symmetric, ν_{sym}, C_2 mode and the asymmetric, ν_{asym}, non-C_2 mode of vibration of the CuN_4Br chromophore. The resulting linear and parallel structural pathways are consistent with the *direct* observation of the effect of vibronic coupling on the stereochemistries of the complexes, which can range from near regular trigonal bipyramidal (RTB) to TBDSBP for the cation distortion isomers of the $[Cu(phen)_2Br][Y]$ complexes.

Introduction

The $[Cu(bipy)_2X][Y]$ (bipy = 2,2′-bipyridine) complexes form a well-established structural pathway,[1,2] where X = Cl^-, Br^- and I^-, Figure 1. This approach has been extended to the eight $[Cu(phen)_2Cl][Y]$ (phen = 1,10-phenanthroline) complexes[3] which show the largest range of stereochemistries[4] (τ = 0.81−0.19) for the $[Cu(chelate)_2X][Y]$ complexes, where chelate = bipy and phen, and $\tau = (\alpha_8 - \alpha_1)/60$[5] , where τ = 1.0 for the regular trigonal bipyramidal (RTB) and τ = 0.0 for a regular square based pyramidal (RSBP) stereochemistry. To date, $[Cu(phen)_2Br][ClO_4]$, **6**,[6] is the only $[Cu(phen)_2Br][Y]$ complex of known crystal structure. In order to examine the range of stereochemistries observed and to establish the directions of the distortion present, this paper reports the crystal structures and electronic properties of five new $[Cu(phen)_2Br][Y]$ complexes, **1**−**5**.

Experimental Section

Preparations. $[Cu(phen)_2Br][Br]\cdot H_2O$, **1**, was prepared by adding a hot solution of phen (0.36 g, 2 mmol) in 200 cm^3 of propanone to a hot aqueous solution (20 cm^3) of $CuBr_2$ (0.22 g, 1 mmol). Hexagonal green crystals of **1** were formed after 3 days. Anal. Calcd for $C_{24}H_{18}CuBr_2N_4O$ (%): C, 47.90; H, 3.01; N, 9.31; Br, 26.56; Cu, 10.56. Found: C, 47.44; H, 2.95; N, 9.26; Br, 26.59; Cu, 10.12. $[Cu(phen)_2Br][ClO_4]$, **2**, was prepared by adding a hot solution of phen (0.36 g, 2 mmol) in 150 cm^3 of propanone to a hot aqueous solution (30 cm^3) of $[Cu(OH_2)_6][ClO_4]_2$ (0.37 g, 1 mmol). Hexagonal green crystals of **2** were formed overnight. Anal. Calcd for $C_{24}H_{16}CuBrN_4ClO_4$ (%): C, 47.78; H, 2.67; N, 9.29; Cu, 10.53. Found (%): C, 47.39; H, 2.53; N, 9.17; Cu, 10.36. $[Cu(phen)_2Br][NO_3]\cdot H_2O$, **3**, was prepared by adding a hot solution of phen (0.72 g, 4 mmol) in 30 cm^3 of ethanol to a hot aqueous solution (30 cm^3) of $Cu(NO_3)_2\cdot 3H_2O$ (0.24 g, 1 mmol) and $CuBr_2$ (0.22 g, 1 mmol). Hexagonal green crystals of **3** were deposited after 5 days. Anal. Calcd for $C_{24}H_{18}CuBrN_5O_4$ (%): C, 49.37; H, 3.11; N, 12.00; Br, 13.69; Cu, 10.89. Found (%): C, 48.95; H, 3.15; N, 11.87; Br, 14.13; Cu, 11.00. $[Cu(phen)_2Br][PF_6]$, **4**, was prepared by adding a hot solution of phen (0.36 g, 2 mmol) in 150 cm^3 of propanone to a hot aqueous solution (30 cm^3) of $Cu(NO_3)_2\cdot 3H_2O$ (0.24 g, 1 mmol) and NaBr (0.10 g, 1 mmol). A hot aqueous solution (20 cm^3) of KPF_6 (0.18 g, 1 mmol) was then added to the mixture. Needle-like green crystals of **4** formed overnight. Anal. Calcd for $C_{24}H_{16}CuBrN_4PF_6$ (%): C, 44.43; H, 2.49; N, 8.64; Br, 12.32; Cu, 9.79. Found (%): C, 44.70; H, 2.51; N, 8.68; Br, 12.53; Cu, 9.39. $[Cu(phen)_2Br][BPh_4]$, **5**, was prepared by adding a hot solution of phen (0.36 g, 2 mmol) in 300 cm^3 of acetonitrile to a hot aqueous solution (30 cm^3) of $CuBr_2$ (0.22 g, 1 mmol). A hot aqueous solution (20 cm^3) of $NaBPh_4$ (0.34 g, 1 mmol) was then added to the mixture. Large olive green crystals of **5** were obtained after 3 days. Anal. Calcd for $C_{48}H_{36}CuBrN_4B$ (%): C, 70.04; H, 4.41; N, 6.81; Br, 9.71; Cu, 7.72. Found (%): C, 70.39; H, 4.42; N, 6.68; Br, 9.49; Cu, 7.72.

Crystallography. The crystallographic and refinement data for **1**−**5** are given in Table 1. The unit cell parameters of **1**−**5** were determined (25 reflections, θ = 3−25°) and their intensities collected on an Enraf-Nonius CAD4 diffractometer. Reflections in the range 3.0 < θ < 24° were collected, in one hemisphere for **1**, **3**, and **5** and in one quadrant for **2** and **4**. The data were collected at room temperature using an $\omega-2\theta$ scan mode and a constant scan speed of 7 deg min^{-1}, with a

† Present address: School of Chemical Sciences, Dublin City University, Dublin 9, Ireland.

⊗ Abstract published in *Advance ACS Abstracts*, December 15, 1997.

(1) Harrison, W. D.; Kennedy, D. M.; Ray, N. J.; Sheahan, R.; Hathaway, B. J. *J. Chem. Soc., Dalton Trans.* **1981**, 1556.
(2) Nagle, P.; O'Sullivan, E.; Hathaway, B. J.; Muller, E. *J. Chem. Soc., Dalton Trans.* **1990**, 3399.
(3) Murphy, G.; Nagle, P.; Murphy, B.; Hathaway, B. J. *J. Chem. Soc., Dalton Trans.* **1997**, 2645.
(4) Brophy, M.; Murphy, G.; O'Sullivan, C.; Hathaway, B. J.; Murphy, B. *Polyhedron*, submitted for publication.
(5) Addison, A. W.; Nageswara Rao, T.; Reedjik, J.; van Rijn, J.; Verschoor, G. C. *J. Chem. Soc., Dalton Trans.* **1984**, 1349.
(6) Parker, O. J.; Greiner, G. T.; Breneman, G. L.; Willett, R. D. *Polyhedron* **1994**, *2*, 267.

S0020-1669(97)00458-8 CCC: $15.00
Published on Web 01/26/1998

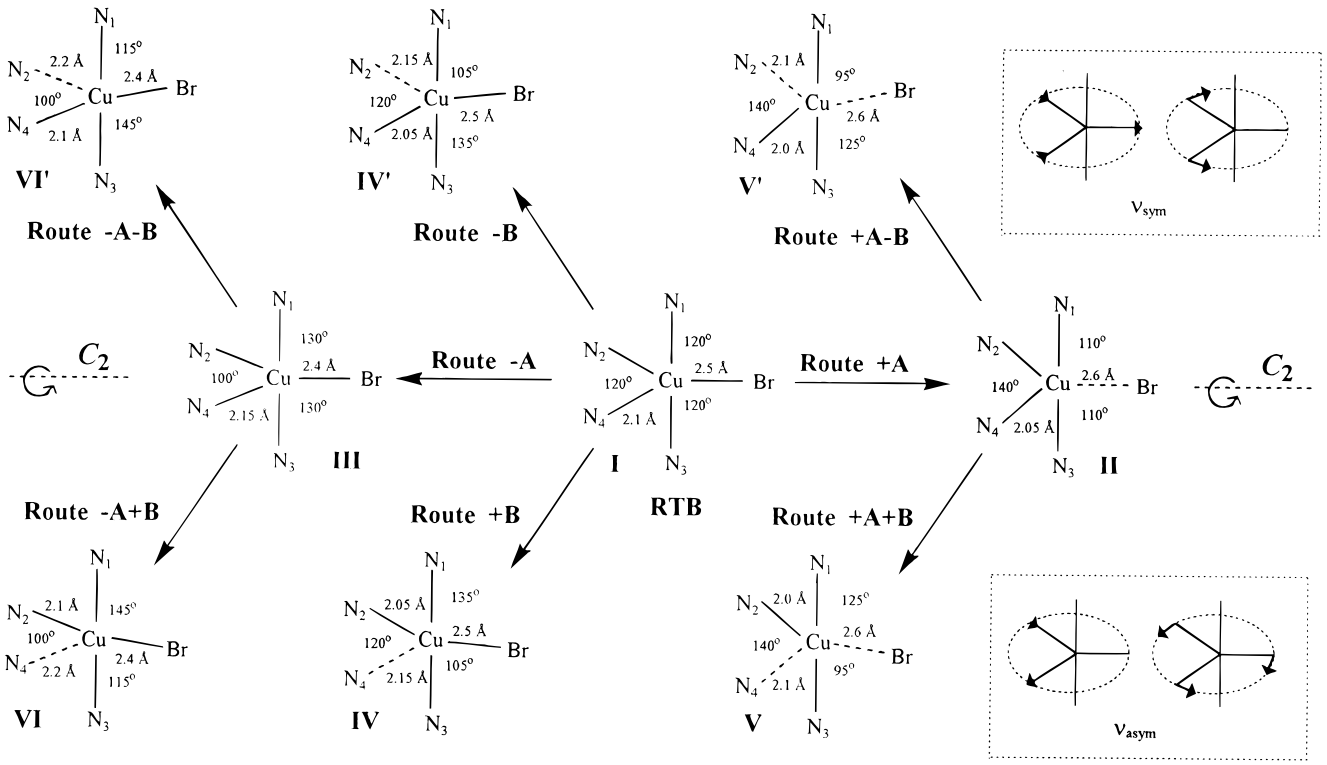

Figure 1. Forms of distortion of the RTB CuN_4Br chromophore involving the ±A, ±B, and ±A ± B routine distortions.[2] (The bond distance values have been rounded off to the nearest 0.05 Å.)

Table 1. Crystallographic and Structure Refinement Data for [Cu(phen)$_2$Br][Br]·H$_2$O, **1**, [Cu(phen)$_2$Br][ClO$_4$], **2**, [Cu(phen)$_2$Br][NO$_3$]·H$_2$O, **3**, [Cu(phen)$_2$Br][PF$_6$], **4**, and [Cu(phen)$_2$Br][BPh$_4$], **5**

	1	**2**	**3**	**4**	**5**
stoichiometry	$C_{24}H_{18}CuBr_2N_4O$	$C_{24}H_{16}CuBrN_4ClO_4$	$C_{24}H_{18}CuBrN_5O_4$	$C_{24}H_{16}CuBrN_4PF_6$	$C_{48}H_{36}CuBrN_4B$
MW	601.793	603.318	583.888	648.831	823.104
cryst syst	triclinic	monoclinic	triclinic	monoclinic	triclinic
space group	$P\bar{1}$ (C_i^1, No. 2)	$P2_1/n$ (C_{2h}^5, No. 14)	$P\bar{1}$ (C_i^1, No. 2)	$P2_1/n$ (C_{2h}^5, No. 14)	$P\bar{1}$ (C_i^1, No. 2)
a (Å)	9.853(1)	10.272(1)	9.929(2)	10.437(2)	11.202(3)
b (Å)	11.363(2)	12.724(2)	11.312(2)	12.533(4)	11.313(3)
c (Å)	11.875(1)	17.450(2)	12.056(2)	18.047(2)	15.738(6)
α (deg)	67.56(1)	90.00	67.03(1)	90.00	86.87(2)
β (deg)	67.35(1)	102.70(1)	68.91(1)	102.32(1)	76.39(2)
γ (deg)	72.09(1)	90.00	71.60(1)	90.00	79.84(2)
V (Å^3)	1113.82	2225.05	1136.75	2306.29	1907.90
Z	2	4	2	4	2
D_c (g cm^{-3})	1.79	1.76	1.71	1.87	1.43
μ (cm^{-1})	44.91	28.58	26.88	27.38	16.06
R^a	0.0601	0.0485	0.0642	0.0535	0.0489
$R_w{}^b$	0.0598	0.0479	0.0628	0.0554	0.0534

^{a} $R = \sum(|F_o| - |F_c|)/\sum|F_o|$. ^{b} $R_w = \{\sum[w(|F_o| - |F_c|)^2/\sum w|F_o|^2]\}^{1/2}$.

variable scan width of (0.8 + 0.2 tan θ). Lorentz and polarization corrections were applied, but no correction was made for absorption. Data reduction was carried out using the program XCAD.[7]

The structures were solved using the SHELX 76[8] and SHELXS 86[9] programs, developed by difference Fourier techniques and refined by full-matrix least-squares analysis. In each case, the least-squares calculations were on $|F|$, the function minimized being $\sum w(|F_o| - |F_c|)^2$. A refined weighting scheme of the form $w = k/[\sigma^2(F_o) + g(F_o)^2]$ was used. Anisotropic thermal parameters were employed for all of the non-hydrogen atoms. The positions of the hydrogen atoms were calculated geometrically and "*floated*" on the appropriate carbon atom positions, assuming C−H distances of 1.08 Å and fixed thermal parameters of 0.07 Å^2. Complex atom scattering factors were used for the non-hydrogen atoms.[10]

For **3**, the anisotropic thermal parameters of $[NO_3]^-$ were high and the maximum residual electron densities were associated with it. The anion was refined as a rigid body, by fixing the N−O distances at 1.226 Å and the O−N−O angles at 120°. A final difference Fourier map revealed no peaks greater than +0.92 and −1.21 e Å^{-3}, which were associated with the $[NO_3]^-$.

(7) McCardle, P. *XCAD, program for data reduction of CAD4 output*; University College Galway: Galway, Ireland, 1990.
(8) Sheldrick, G. M. *SHELX 76, program for X-ray crystal structure determination*; University of Cambridge: Cambridge, U.K., 1976.
(9) Sheldrick, G. M. *SHELXS 86, program for X-ray crystal structure solution*; University of Göttingen: Göttingen, Germany, 1986.
(10) Cromer, D. T.; Waber, J. T. *International Tables of Crystallography*; Kynoch Press: Birmingham, U.K., 1974; Vol. IV, pp 71, 148. (Present distributor Kluwer Academic Publishers, Dordrecht, The Netherlands.)
(11) Roberts, P.; Sheldrick, G. M. *XANADU, program for the calculation of crystallographic data*; University of Cambridge: Cambridge, U.K., 1979.
(12) Henrick, K. *PUBTAB, program to prepare and print crystallographic tables for publication*; University of North London: London, 1980.
(13) Spek, A. L. *PLUTON-92, program to prepare and print molecular structures*; University of Utrecht: Utrecht, The Netherlands, 1992.

Table 2. Selected Bond Lengths (Å) and Bond Angles (deg) for the $[Cu(phen)_2Br][Y]$ and $[Cu(phen)_2I][Y]$ Complexes

	Br						I		
	$Y = ClO_4$ (**6**[6])	$Y = Br{\cdot}H_2O$ (**1**)	$Y = ClO_4$ (**2**)	$Y = NO_3{\cdot}H_2O$ (**3**)	$Y = PF_6$ (**4**)	$Y = BPh_4$ (**5**)	$I{\cdot}^3/_4H_2O$ (**7**[15])	$Y = PF_6$ (**8**[16])	$Y = I{\cdot}S_8$ (**9**[17])
Cu−Cl(X)*	2.356(1)	2.331(1)	2.373(1)	2.312(1)	2.364(1)	2.258(1)	2.389(1)	2.369(2)	2.342(5)
Cu−X	2.496(1)	2.471(1)	2.513(1)	2.452(1)	2.504(1)	2.398(1)	2.719(1)	2.699(2)	2.672(5)
Cu−N(1)	1.985(5)	1.978(4)	1.981(4)	1.997(4)	1.987(4)	2.025(3)	1.962(7)	1.998(7)	2.000(10)
Cu−N(2)	2.091(3)	2.072(4)	2.095(4)	2.085(3)	2.088(4)	2.055(3)	2.089(7)	2.086(7)	2.100(10)
Cu−N(3)	1.985(5)	1.978(4)	2.002(4)	2.002(4)	1.996(4)	1.997(3)	1.946(7)	1.998(7)	2.000(10)
Cu−N(4)	2.091(3)	2.086(4)	2.101(4)	2.108(3)	2.126(4)	2.217(3)	2.240(7)	2.086(7)	2.100(10)
α_1	119.8(1)	126.5(1)	125.7(1)	129.8(1)	133.4(1)	157.2(1)	115.4(2)	122.3(2)	125.3(3)
α_2	119.8(1)	120.1(1)	110.0(1)	120.9(1)	105.1(1)	105.9(1)	127.3(2)	122.3(2)	125.3(3)
α_3	120.6(2)	113.5(2)	124.3(1)	109.3(1)	121.5(2)	96.8(1)	117.2(2)	115.4(2)	109.4(3)
α_4	91.5(1)	91.0(1)	91.7(1)	91.7(1)	92.3(1)	93.3(1)	91.3(2)	91.5(2)	92.3(3)
α_5	91.5(1)	90.5(1)	90.9(1)	91.3(1)	91.4(1)	91.0(1)	89.8(2)	91.5(2)	92.3(3)
α_6	81.1(2)	81.9(2)	80.9(2)	81.5(1)	81.2(2)	81.2(1)	79.6(3)	81.9(3)	80.4(4)
α_7	81.1(2)	82.0(2)	81.6(2)	81.5(1)	81.0(2)	79.8(1)	81.7(3)	81.9(3)	80.4(4)
α_8	177.0(2)	178.4(2)	177.2(2)	177.1(1)	176.3(2)	170.2(1)	178.9(3)	176.9(3)	175.5(4)
α_9	97.5(2)	97.5(2)	98.3(2)	96.6(1)	96.6(2)	91.5(1)	100.3(3)	96.5(2)	97.0(4)
α_{10}	97.5(2)	96.8(2)	96.6(2)	97.0(1)	97.6(2)	107.4(1)	97.5(3)	96.5(2)	97.0(4)
τ	0.95	0.87	0.86	0.79	0.72	0.22	1.06	0.91	0.84

[a] The Cu−X distances are corrected to Cu−Cl values using the following relationships: Cu−Br - 0.14 Å = Cu−Cl(Br) and Cu−I - 0.33 Å = Cu−Cl(I).

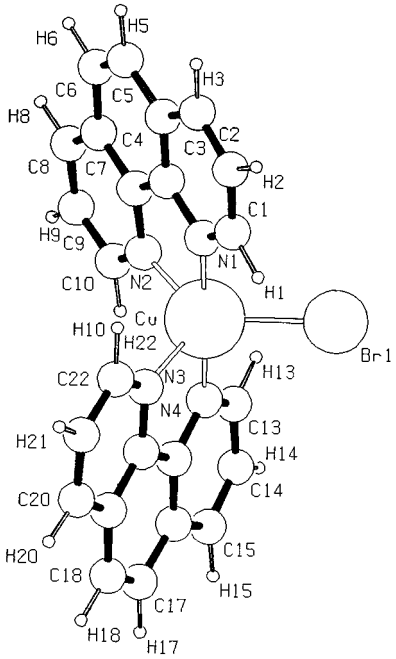

Figure 2. Molecular structure of $[Cu(phen)_2Br]^+$ of **1**.

All calculations were carried out using the SHELX 76,[8] SHELXS 86,[9] XANADU,[11] PUBTAB,[12] and XCAD[7] programs on a VAX 6310 computer. PLUTON-92[13] was run on a Memorex 386 PC.

Selected bond lengths and bond angles for the six $[Cu(phen)_2Br][Y]$ complexes are given in Table 2. Figure 2 shows a representative molecular structure for the $[Cu(phen)_2Br]^+$ cation of **1**, and Figure 3 shows the atomic numbering scheme and the angular notation used.

The diffuse reflectance spectra in the range 5000−30 000 cm^{-1}, were measured as polycrystalline samples on a Shimadzu UV−vis 3101 spectrometer.

The additional material, available from the Cambridge Crystallographic Data Centre, comprises the final fractional atomic coordinates, the anisotropic thermal parameters, the full bond length and angle data, and selected mean plane data.

Results and Discussion

Crystal Structures. The crystal structures of **1**−**5** consist of discrete $[Cu(phen)_2Br]^+$ cations, $[Br]^-$, $[ClO_4]^-$, $[NO_3]^-$, $[PF_6]^-$, and $[BPh_4]^-$ anions, respectively, and H_2O molecules for **1** and **3**. None of the anions or water molecules are close enough (<3.0 Å) to be considered even weakly semicoordinated to the copper(II) cation.[14] The cations all involve a five coordinate CuN_4Br chromophore in a general position, with a near trigonal bipyramidal stereochemistry having a square based pyramidal distortion[2] (SBPDTB) in **1**−**4** and a trigonal bipyramidal distorted square based pyramidal stereochemistry (TBDSBP) in **5**. These five complexes are further examples of distortion isomers of the $[Cu(phen)_2X]^+$ cation,[3,6] whose stereochemistries are related by the structural pathways[1,3] of Figure 1. No attempt will be made to describe the individual structures of complexes **1**−**5**, Table 2, but scatter plot analysis will be used to compare their structures with that of $[Cu(phen)_2Br][ClO_4]$, **6**, the only $[Cu(phen)_2Br][Y]$ complex to date of known crystal structure.[6] Table 2 summarises the selected bond lengths and bond angles of the six $[Cu(phen)_2Br][Y]$ complexes, sequenced in order of their τ values, where $\tau = (\alpha_8-\alpha_1)/60$.[5] Compound **6**[6] differs from complexes **1**−**5**, as the Cu and Br atoms lie on a 2-fold axis of symmetry. There are three $[Cu(phen)_2I][Y]$ complexes of known crystal structure,[15−17] with two complexes having a 2-fold axis of

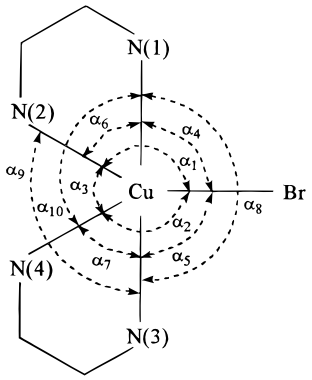

α_1 = N(2) - Cu - Br
α_2 = N(4) - Cu - Br
α_3 = N(4) - Cu - N(2)
α_4 = N(1) - Cu - Br
α_5 = N(3) - Cu - Br
α_6 = N(2) - Cu - N(1)
α_7 = N(4) - Cu - N(3)
α_8 = N(3) - Cu - N(1)
α_9 = N(3) - Cu - N(2)
α_{10} = N(4) - Cu - N(1)

Figure 3. Atomic numbering scheme and α_n notation for the CuN_4Br chromophore.

(14) Procter, I. M.; Hathaway, B. J.; Nichols, P. *J. Chem. Soc., A* **1968**, 1678.
(15) Nagle, W. P. Ph.D. Thesis, National University of Ireland, 1990.
(16) Harrington, C.; Hathaway, B. J. Unpublished results.

Table 3. Selected Bond Lengths (Å) and Bond Angles (deg) for the [Cu(phen)$_2$Cl][Y] Complexes

	Y = $BF_4 \cdot {}^1/_2H_2O$ (**10**[15])	Y = ClO_4 (**11**[23])	Y = PF_6 (**12**[15])	Y = $Cl \cdot 1^1/_2H_2O \cdot (CH_3)_2CO$ (**13**[24])	Y = $NO_3 \cdot H_2O$ (**14**[25])	Y = $Cl \cdot 1^1/_2H_2O \cdot (CH_3)_2CO$ (**15**[24])	Y = $CF_3SO_3 \cdot H_2O$ (**16**[26])	Y = BPh_4 (**17**[26])
Cu−Cl	2.304(2)	2.298(2)	2.294(2)	2.281(1)	2.292(1)	2.257(1)	2.280(1)	2.254(1)
Cu−N(1)	1.995(6)	1.986(6)	2.001(4)	1.999(4)	1.988(4)	1.990(4)	1.998(2)	2.024(2)
Cu−N(2)	2.078(5)	2.077(6)	2.076(4)	2.126(3)	2.091(2)	2.108(2)	2.127(2)	2.057(2)
Cu−N(3)	2.011(6)	2.004(6)	2.003(4)	1.995(3)	1.989(4)	1.993(4)	1.996(2)	2.008(2)
Cu−N(4)	2.121(6)	2.136(6)	2.157(4)	2.138(3)	2.132(2)	2.151(4)	2.151(2)	2.242(2)
α_1	126.6(2)	127.6(2)	131.6(1)	130.4(1)	135.8(1)	133.0(1)	138.7(1)	157.7(1)
α_2	118.9(2)	119.0(2)	114.4(1)	129.6(1)	119.2(1)	120.6(1)	127.9(1)	105.9(1)
α_3	114.5(2)	113.4(2)	114.1(2)	100.0(1)	105.0(1)	106.4(1)	93.4(1)	96.4(1)
α_4	92.8(2)	92.3(2)	93.4(1)	94.1(1)	92.7(1)	96.8(1)	93.2(1)	92.7(1)
α_5	91.2(2)	90.9(2)	91.0(1)	95.0(1)	91.8(1)	94.2(1)	94.6(1)	91.4(1)
α_6	81.3(2)	81.7(2)	81.0(2)	80.1(2)	81.4(1)	81.1(1)	80.7(1)	81.0(1)
α_7	80.6(2)	80.5(2)	80.1(2)	80.5(1)	80.8(1)	80.6(2)	80.2(1)	79.2(1)
α_8	175.3(2)	176.2(2)	175.2(2)	170.8(1)	175.6(1)	168.6(2)	172.1(1)	169.2(1)
α_9	98.1(2)	98.2(2)	97.5(2)	95.1(2)	95.8(1)	93.8(1)	92.8(1)	91.5(1)
α_{10}	95.4(2)	96.0(2)	96.3(2)	92.5(1)	96.5(1)	91.0(2)	95.7(1)	109.1(1)
τ	0.81	0.81	0.73	0.67	0.66	0.59	0.56	0.19

symmetry,[16,17] Table 2. The chromophore of **6**, has a near RTB stereochemistry, with $\tau = 0.95$. The structures of **6** and **2** are two independent isomers of the [Cu(phen)$_2$Br][ClO_4] complex. The X-ray crystal structure determinations were carried out in different space groups, monoclinic and triclinic, respectively, which were checked to confirm that **6** and **2** were not identical. The structural data show that **6** has a 2-fold axis of symmetry, while **2** does not, with differences in bond lengths and angles of $\sim$ 0.02 Å and $\sim$ 10° and τ values of 0.95 and 0.86, respectively, Table 2.

For the six [Cu(phen)$_2$Br][Y] complexes, the structure of the five coordinate CuN_4Br chromophore varies from near RTB to near SBP, which is reflected in a range of τ values from 0.95 to 0.22, $\Delta = 0.73$. This is the largest range seen to date for any series of five coordinate cation distortion isomers[18] involving the *same* CuN_4X chromophore, with the same set of ligand atoms.[3,18,19] Complex **5** has a τ value of 0.22 and TBDSBP stereochemistry.[20] The remaining four complexes have τ values in the more limited range of 0.87−0.72 and have SBPDTB stereochemistries. The extreme SBPDTB stereochemistry of **5** has been observed previously[3] for a [Cu(phen)$_2$Cl][Y] complex, **17**, with a τ value of 0.19, Table 3. As the extreme structure of **17** has been questioned, the X-ray structure determination has been independently redetermined,[4] with no significantly different results. The repeated data collection was carried at 150 K, confirming that the SBPDTB stereochemistry of **17** is a static stereochemistry[20] of the copper(II) cation and is not a consequence of a temperature variable behavior.

Complexes **2** and **4** are the first [Cu(phen)$_2$X][Y] complexes, where X = Cl^-, Br^-, and I^-, to show α_3 values slightly >120° at 124.3(1) and 121.5(2)°, respectively, suggesting that a small +A route distortion is occurring. This behavior has also been seen for four [Cu(bipy)$_2$Cl][Y] complexes.[1,2]

From Table 2 it is noticeable that within the range of τ values of 0.22−0.95 there is a significant gap of 0.50 in τ value between the extreme TBDSBP value of 0.22 for **4** and the next highest value of 0.72 for **4**. This gap corresponds with a change in the ratio of the α_9 and α_{10} angles, for τ values >0.72, $\alpha_9 > \alpha_{10}$, but, for τ values <0.72, $\alpha_9 < \alpha_{10}$. Equally, while the phen ligand is constrained to be essentially planar, with angles between the pyridine rings of 0−5°, in **5** both of these angles are less than 1.02°. This suggests that the geometry of the TBDSBP stereochemistry is inherently more stable, once formed, than the range of SBDTB stereochemistries 0.72−0.95, a stability that could be locked in place by the essential planarity of the phen ligand. This is also reflected in the near trigonal α_1 angles of 119.8−133.4° of the SBPDTB stereochemistries, relative to an α_1 angle of 157.2° in **4**.

Table 4. Suggested Limiting Values for the ±A, +B, −A + B, and +A + B Route Distortions

	RTB	+A	−A	+B	−A + B	+A + B
α_1/deg	120	97.5	135	150	165	105
α_2/deg	120	97.5	135	90	105	90
α_3/deg	120	165	90	120	90	165
Cu−N(2)/Å	2.092	1.998	2.155	1.985	2.048	1.971
Cu−N(4)/Å	2.092	1.998	2.155	2.199	2.262	2.025
Cu−Br/Å	2.494	2.683	2.368	2.494	2.368	2.683

General Principles for the Scatter Plot Analysis of the [Cu(phen)$_2$Br][Y] Complexes. The surprising feature of the data of Table 2 is the range in the τ values, the Cu−Br, Cu−N(2), and Cu−N(4) distances and the α_1, α_2, and α_3 angles. A general discussion of the use of scatter plots has been given earlier[3] and will now be applied to the $[Cu(phen)_2Br]^+$ cation. Data point **6** not only has a 2-fold axis of symmetry, but also is the nearest experimental data point to the assumed RTB data point, which has $\alpha_1 = \alpha_2 = \alpha_3 = 120°$, Cu−N(2,4) distances of 2.092 Å, and a Cu−Br distance of 2.494 Å, Table 4. The notation Cu−N(2,4) is used to represent the equivalence of the Cu−N(2) and Cu−N(4) distances, due to the 2-fold axis of symmetry. The factors limiting the in-plane angular distortion from RTB are that the α_1, α_2, and α_3 angles generally have values >90° and <180°, and the sum of the in-plane angles is a constant, $\alpha_1 + \alpha_2 + \alpha_3 = 360°$, Table 5. A constant value for the sum of the in-plane bond lengths might also be expected but is not subject to a geometrical constraint. However, Table 5 shows the values ranging from 6.629 to 6.718 Å, $\Delta = 0.089$ Å, and they differ significantly from the RTB sum, 6.678 Å. The Cu−N(2,4) distances are constrained by the bite of the chelate ligand, whereas the Cu−Br distance has no constraint of this type, which may explain why the in-plane distances do not have an exactly constant value for the sum. Thus, the results are more variable for the distance plots.[21]

(17) Hambley, T. W.; Raston, C. L.; White, A. H. *Aust. J. Chem.* **1977**, *30*, 1965.
(18) Ray, N. J.; Hulett, L.; Sheahan, R.; Hathaway, B. J. *J. Chem. Soc., Dalton Trans.* **1981**, 1463.
(19) Hathaway, B. J. *Struct. Bonding (Berlin)* **1984**, *57*, 55.
(20) Hathaway, B. J.; Billing, D. E. *Coord. Chem. Rev.* **1970**, *5*, 143.
(21) Murphy, G.; Murphy, C.; Murphy, B.; Hathaway, B. J. *J. Chem. Soc., Dalton Trans.*, submitted for publication.

Table 5. Sums of (a) the In-Plane Bond Angles and (b) the In-Plane Bond Distances for the $[Cu(phen)_2Br][Y]$ Complexes

	6	**1**	**2**	**3**	**4**	**5**
α_1/deg	119.8	126.5	125.7	129.8	133.4	157.2
α_2/deg	119.8	120.1	110.0	120.9	105.1	105.9
α_3/deg	120.6	113.5	124.3	109.3	121.5	96.8
(a) sum/deg	360.2	360.1	360.0	360.0	360.0	359.9
Cu−N(2)/Å	2.091	2.072	2.095	2.085	2.088	2.055
Cu−N(4)/Å	2.091	2.086	2.101	2.108	2.126	2.217
Cu−Br/Å	2.496	2.471	2.513	2.452	2.504	2.398
(b) sum/Å	6.678	6.629	6.709	6.645	6.718	6.670

Figure 1 illustrates the eight general stereochemistries arising from the ±A and ±B senses of distortion of the RTB CuN_4Br chromophore.[2] The values of the bond distances and angles in Figure 1 are experimental values (rounded off to the nearest 0.05 Å) obtained from the $[Cu(chelate)_2X][Y]$ complexes.[2] The +A and +A ± B route distortions yield stereochemistries distorted toward SBP, with the axial elongation along the Cu−Br direction. The −A, +B, and −A ± B route distortions also yield SBP distorted stereochemistries, with the axial elongation along the Cu−N(4) or the Cu−N(2) directions. Complex **6**[6] is the only complex with a 2-fold axis of symmetry, and with α_3 > 120° (120.6°) and Cu−Br > 2.494 Å (2.496 Å), it shows a slight +A route distortion. The remaining five complexes do not have a 2-fold axis of symmetry, suggesting that the routes operate in combination, ±A ± B. In order to compare the Cu−Br distances with the Cu−N(1−4) distances, they are corrected for the difference in the Br and N atom covalent radii, namely, 0.43 Å. If the Cu−Br distances are adjusted to Cu−N values,[22] using the relation Cu−Br - 0.43 Å = Cu−N(Br), Table 2, it can be seen that the greatest elongation of the equatorial distances is in the Cu−N(4) direction, indicating a +B route distortion. Simultaneously, the α_3 values decrease <120°, and the Cu−Br distances also decrease, indicating a −A route distortion. This suggests that +A, −A + B, and +A + B route distortions operate for the $[Cu(phen)_2Br][Y]$ series of complexes; however, the +A route distortion is only small.

The suggested limiting values[3,21] for the ±A, +B, and ±A + B route distortions are illustrated in Table 4. The angle *versus* angle plots and the distance *versus* distance plots can be divided up to represent ±A, ±B axes and ±A ± B sections, Figure 4a−d. The limiting values for the −B, −A − B, and +A − B route distortions are equivalent to those for +B, −A + B, and +A + B, respectively, since each pair (±B, −A ± B, and +A ± B) are related by a 2-fold axis of symmetry.

Scatter Plot Analysis of the $[Cu(phen)_2Br][Y]$ Complexes. The data of the $[Cu(phen)_2Br][Y]$ complexes, Table 2, are presented in this section using scatter plot analysis. Each plot includes not only the $[Cu(phen)_2Br][Y]$ data points but also the $[Cu(phen)_2Cl][Y]$ and $[Cu(phen)_2I][Y]$ data points, Tables 2 and 3, for later comparison, with the Cu−Br and Cu−I distances corrected, by the difference in their covalent radii, to the corresponding Cu−Cl distance.[22] The scatter plots to be discussed, using the in-plane bond lengths and angles, are as follows: (a) τ *versus* Cu−N(4), (b) α_3 *versus* α_1, (c) α_3 *versus* Cu−Br*, and (d) Cu−Br* *versus* Cu−N(2). Figure 4a provides an overview of the range of stereochemistries defined by the τ value. Since this parameter involves two simultaneous angle changes, α_1 and α_8, it will not be used further. The six data points vary from near RTB to near RSBP (−A + B), with the τ values decreasing from 0.95 to 0.22 as the Cu−N(4) distances increase from 2.086(4) to 2.217(3) Å. This plot provides a qualitative indication of the range of the observed stereochemistries of the $[Cu(phen)_2Br][Y]$ complexes. There is one data point, **6**, at near RTB, with τ = 0.95. Four data points have τ values ranging from 0.87 to 0.72, with stereochemistries best described as SBPDTB. Data point **5** has an exceptionally low τ value of 0.22 at near RSBP. There are no data points lying on the RTB → RSBP pathway. Three data points, **2**−**4**, lie on a parallel correlation, with the remaining three data points, **1**, **5**, and **6** lying nearby. Figure 4b: The data points show the α_3 values decreasing from 124.3(1) to 96.8(1)° as the α_1 values increase from 119.8(1) to 157.2(1)°. All six data points have α_1 values > 119.8°, but with α_3 values > 120°, for **6**, **2**, and **4**, and <120°, for **1**, **3**, and **5**. The sum of the in-plane angles gives a constant value, $\alpha_1 + \alpha_2 + \alpha_3 = 360°$, Table 5. The ±A and ±B axes are superimposed on the graph. The data points lie in three different sections. Data point **6** is very close to RTB, but it lies slightly along the +A pathway. Three data points, **1**, **3**, and **5**, are found in the −A + B section of the graph. The remaining two data points, **2** and **4**, are present in the +A + B section. There are no data points lying on the RTB → RSBP (−A + B) pathway. Three data points, **1, 3**, and **6**, show an *inverse* trend through the RTB data point. Each of these data points have α_2 values of 120 ± 1°. The remaining three data points, **2**, **4**, and **5**, lie on two possible parallel correlations displaying α_2 values of 110 and 105°, respectively. This series of three possible parallel correlations have the same slopes. The data points show a SBP distortion, but only with an α_2 value of 105° can the correlation end up at RSBP. For each parallel correlation, the α_2 values remain essentially constant; therefore $\Delta\alpha_1\uparrow \approx \Delta\alpha_3\downarrow$, as $\alpha_1 + \alpha_2 + \alpha_3 = 360°$. Table 6 shows the % ±A and % +B distortion values of the six $[Cu(phen)_2Br][Y]$ complexes calculated using the in-plane α_3 and α_1 angle data. Figure 4c: The six data points show the α_3 angles decreasing from 124.3(1) to 96.8(1)°, Δ = 27.5°, as the Cu−Br* distances decrease from 2.313(1) to 2.258(1) Å, Δ = 0.115 Å. All six data points lie on a *normal* linear correlation, which is the best linear trend observed to date (correlation coefficient = 0.999), for the $[Cu(chelate)_2X][Y]$ complexes.[1−3] If the suggested extreme ±A data points are superimposed on the graph, the graph can be divided into two sections, +A, where α_3 > 120° and Cu−Br* > 2.354 Å, and −A, where α_3 < 120° and Cu−Br* < 2.354 Å. However, the +A extension, data points, **2**, **4**, and **6**, from RTB is only small, $\Delta\alpha_3$ = 4.3°, relative to the −A extension, data points, **1**, **3**, and **5**, where $\Delta\alpha_3$ = 23.2°. Consequently the $[Cu(phen)_2Br][Y]$ complexes involve a predominantly −A route distortion. Figure 4d: The data points show the Cu−Br* distances decreasing from 2.373(1) to 2.258(1) Å, while the Cu−N(2) distances decrease from 2.095(4) to 2.055(3) Å. Three data points, **2**, **4**, and **6**, have Cu−Br* values slightly > 2.354 Å, with three data points, **1**, **3**, and **5**, having Cu−Br* values significantly < 2.354 Å. Data point **2** has a Cu−N(2) value slightly > 2.092 Å, with the remaining five data points having Cu−N(2) values < 2.092 Å, to give an overall *normal* trend, but with a suggestion of some *inverse* correlations. The ±A and ±B axes can be superimposed on the plot. Two data points, **6** and **4**, lie on the RTB → +A pathway. Data point **2** is present in the +A − B section of the graph. Three data points, **1**, **3**, and **5**, are found in the −A + B section of the graph. Data point **5** lies on the RTB → RSBP (−A + B) pathway.

$[Cu(phen)_2X][Y]$ Complexes, X = Cl^- and I^-. The eight $[Cu(phen)_2Cl][Y]$ complexes **10**−**17**,[3,23−26] Table 3, have been discussed elsewhere.[3] When these data points are added to the

(22) Muller, E.; Piguet, C.; Bernardelli, G.; Williams, A. F. *Inorg. Chem.* **1988**, *27*, 849.

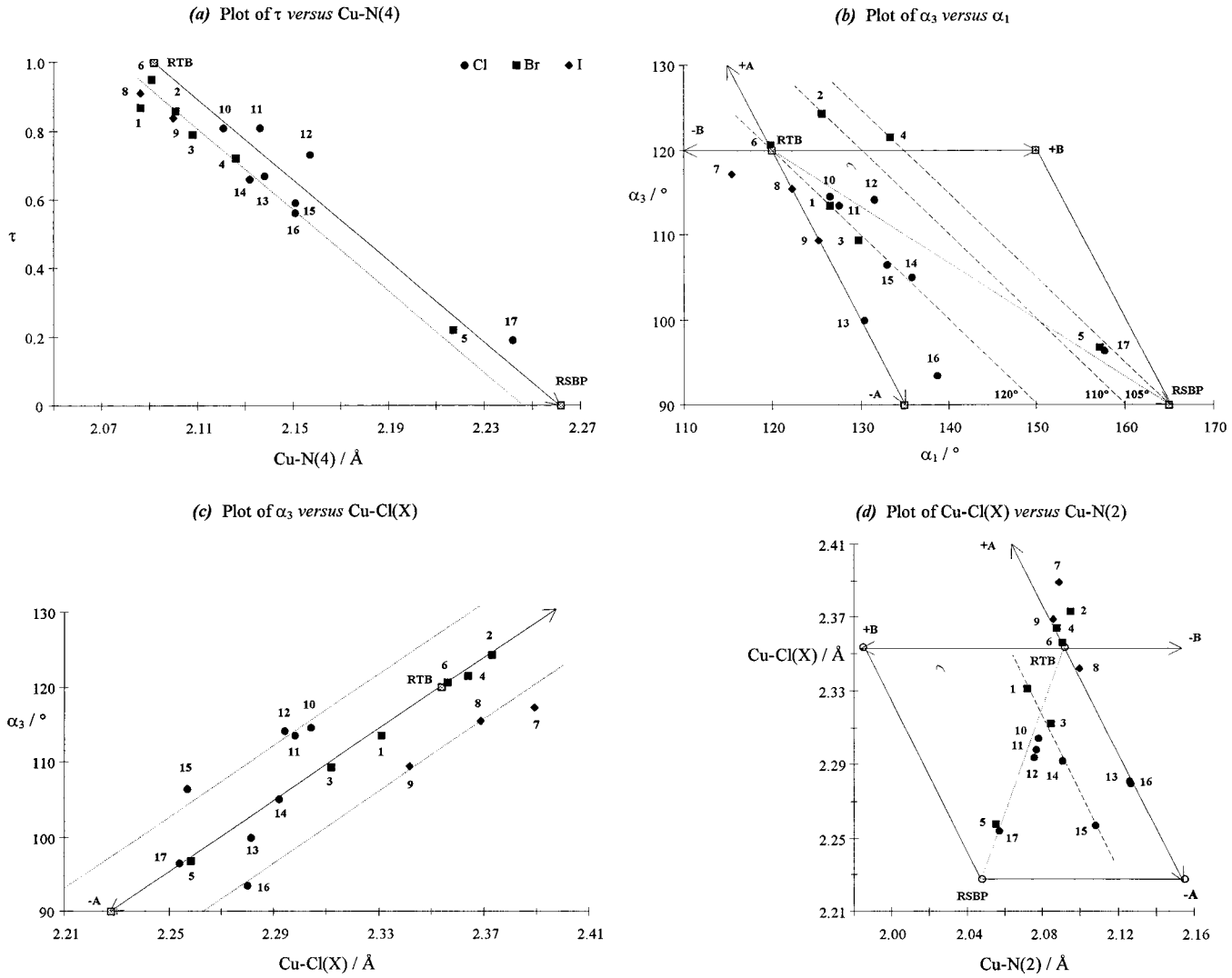

Figure 4. Scatter plots for the [Cu(phen)$_2$X][Y] Complexes.

Table 6. ±A and +B Distortion (%) of the Complexes Calculated Using the In-Plane α_3 and α_1 Angle Data, Figure 4b

	6	**1**	**2**	**3**	**4**	**5**
% −A		21		36		77
% +A	1		10		3	
% +B		11	26	15	47	86

scatter plots of Figure 4a−d, they largely overlap the Br$^-$ data points, with comparable ranges and spread of the data points. The Cl$^-$ data points also have an extreme data point, **17**, with a τ value of 0.19. However, none of the Cl$^-$ complexes involve a 2-fold axis of symmetry. The addition of the eight Cl$^-$ data points to the scatter plots of Figure 4a−b consolidates the trends, and only in the case of the α_3 *versus* Cu−Br* plot, Figure 4c, does the Cl$^-$ data suggest two additional correlations, parallel to the central +A → RTB → −A correlation. Addition of the three [Cu(phen)$_2$I][Y] data points **7**−**9**,[15−17] Table 2, to the scatter plots has a less significant impact as all three data points tend to cluster close to the RTB data point, although still enhancing the linear correlation in Figure 4c and the alternative *inverse* correlation of Figure 4d, through the RTB data point. However, two of the I$^-$ complexes do involve a 2-fold axis of symmetry, Table 2.

Possible Interpretation of the ±A and ±B Route Distortions in Terms of Modes of Vibration. The extensive range of the Cu−L distances and of the α_n angles, Table 3, 0.13 Å and 37°, respectively, have only been interpreted in terms of the ±A and ±B route distortions, Table 6, but it has been suggested earlier[3] that these routes may be understood, alternatively, in terms of the modes of vibration of the CuN_4Br chromophore,[27−30] Figure 5. The symmetric, ν_{sym}, and asymmetric, ν_{asym}, modes of vibration of the CuN_4Br chromophore, Figure 5, both have stretching and bending components. They predict variations in the in-plane parameters, α_{1-3}, Cu−Br, Cu−N(2), and Cu−N(4), which show the largest ranges in distances and angles, Table 2, as ν_{sym} and ν_{asym} modes are largely restricted to the in-plane angles and distances. The symmetric mode of vibration has a 2-fold axis of symmetry, so Cu−N(2) = Cu−N(4) and $\alpha_1 = \alpha_2$, and all six in-plane distances and angles are involved. The asymmetric mode of vibration does not have a 2-fold axis of symmetry. Here only the Cu−N(2) and Cu−N(4) distances and the α_1 and α_2 angles are involved,

(23) Boys, B.; Escobar, C.; Martinez-Carrera, S. *Acta Crystallogr., Sect. B* **1981**, *37*, 351.
(24) Chilkevich, A. K.; Ponomarev, B. P.; Lyavrentjeu P. P.; Atoumjan, L. O. *Koord. Khim.* **1987**, *13*, 1532.
(25) Boys, D. *Acta Crystallogr., Sect. C* **1988**, *44*, 1539.
(26) Murphy, G. Ph.D. Thesis, National University of Ireland, 1997.
(27) Nakamoto, K. *Infrared Spectra of Inorganic and Coordination Compounds*, 3rd ed.; John Wiley and Sons: New York, 1978.
(28) Bacci, M. *J. Chem. Phys.* **1986**, *104*, 191.
(29) Reinen, D.; Atanasov, M. *J. Chem. Phys.* **1989**, *136*, 27.
(30) Reinen, D.; Atanasov, M. *Magn. Reson. Rev.* **1991**, *15*, 167.

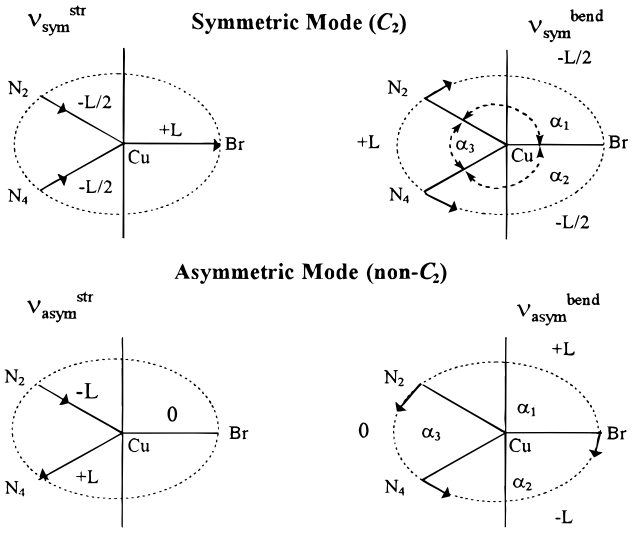

Figure 5. Symmetric and asymmetric modes of vibration for the five coordinate CuN_4Br chromophore, including the relative magnitudes (L).[2,6]

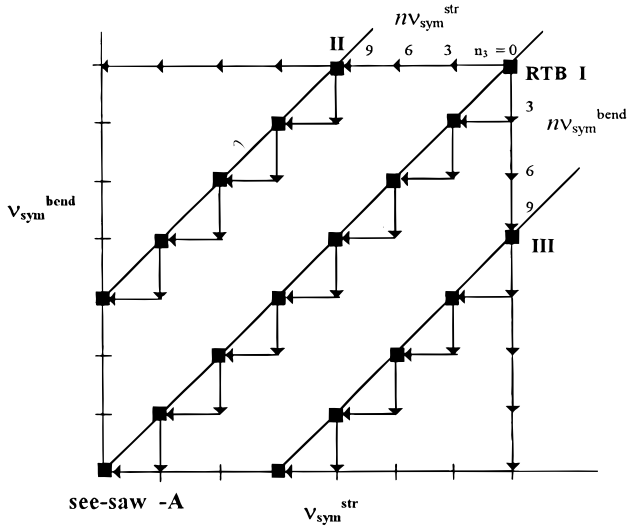

Figure 6. Diagram of how the linear and parallel pathways are formed by the sequential operation of the ν_{sym}^{str} and ν_{sym}^{bend} modes of vibration.

E'' < d_{yz} d_{xz} > E		B_2 B_1	B B	A A
E' < d_{xy} $d_{x^2-y^2}$	B_2 B_1	A_2 A_1	A A	A A
A_1'	d_{z^2}	A_1	A_1	A	A
Symmetry		D_{3h}	C_{4v}	C_{2v}	C_2	C_1
Jahn-Teller Active		No	No	No	No	No
pseudo J. T. ν_{sym} (C_2)		Yes	No	Yes	Yes	Yes
Active ν_{asym} (non-C_2)		No	No	No	No	Yes

Figure 7. One-electron orbital levels of the RTB stereochemistry and their symmetries in various point groups.

with the Cu−Br distance and the α_3 angle being invariant. In the next section, the [Cu(phen)$_2$Br][Y] data of the scatter plot analysis of the in-plane bond lengths and angles are considered to determine if the distribution of data points is alternatively determined by the ν_{sym} and ν_{asym} modes of vibration as the dominant modes of distortion of the CuN_4Br chromophore, Figure 5.

The first problem associated with this suggestion is that the effect of a single mode of vibration of the nuclear framework of the CuN_4X chromophore, of *ca.* 200 cm^{-1}, would only result in bond distance and bond angle changes of 0.005 Å and 1°, respectively.[31] These values are at least an order of magnitude too small to account for the observed changes, Table 2. Consequently, either a progression of 20−40 modes of vibration must be involved or the "amplification factor"[32] of the pseudo-Jahn−Teller effect[33] must be in operation, with the possibility that the former accounts for the latter.

The most convincing evidence for the vibronic coupling model has been seen in accounting for the dynamic *pseudo*-Jahn−Teller distortion[29,30] of the high-symmetry RTB $[CuCl_5]^{3-}$ anion, D_{3h} symmetry, to the lower symmetry RSBP stereochemistry, C_{2v} or C_2 symmetry, with distortion via the ϵ' mode of vibration[29,30] (equivalent to $\nu_{sym}^{str} + \nu_{sym}^{bend}$), with C_2 symmetry along the three in-plane directions at 120° to each other. This requires that the CuN_4Cl chromophore has *effective* symmetry D_{3h} and ignores the presence of non-equivalent donor atoms and the effect of two chelate ligands. If this assumption can be accepted, then the ϵ' mode of vibration, in D_{3h} symmetry, and the ν_{sym}^{str} and ν_{sym}^{bend} modes of vibration (C_2 symmetry) models are equivalent. However, the present authors prefer the ν modes of vibration notation, as it is chemically more intuitive than the ϵ' mode notation. While the authors admit[29,30] that this model is only justified for small distortions, the above "amplification factor"[32] or progressions could equally be operating to account for the larger distortions observed. The highest possible symmetry for the CuN_4Br^* chromophore is C_2, which is restricted to the Cu−Br direction of the CuN_4Br^* chromophore (+A route) and one that is quite distinct from the two ±B route distortions, which are only related by an external 2-fold axis of symmetry. In practice the bulk of CuN_4Br^* chromophores lack any symmetry at all, namely, C_1.

One of the most significant features of Figure 4c is that the six Br$^-$ data points lie strictly along the +A → RTB → −A pathway, suggesting that the changes in the α_3 angle and Cu−Br* distance are closely linked. One such linking process suggests that the changes in these parameters is determined only by the underlying nuclear modes of vibration,[27,28] Figure 5, of a vibronic coupling mechanism.[33] A feature of the parameters of Figure 4c is that the α_3 angle can only be changed by the ν_{sym}^{bend} mode of vibration and the Cu−Br* distance can only be changed by the ν_{sym}^{str} mode of vibration. If such modes operated separately from RTB, point **I** in Figure 6, the former would only produce a vertical linear correlation of data points and the latter a horizontal correlation. While such limited correlations can be identified in Figure 4c, the most convincing correlation of six data points occurs at an angle of 34° to the Cu−Br* axis. The only way such a positive correlation can occur is if the two modes of vibration are strongly coupled together (they both transform as A in C_1 symmetry, Figure 7), as shown in Figure 6, to produce a stepped displacement. However, such a single displacement due to one quantum of each mode of vibration would still be too small to be observed on the scale of Figure 4c, namely, 0.005 Å and 1°.[31] For the scale of the +A → RTB → −A pathway in Figure 4c to be observed, a change of 0.13 Å in the Cu−Br* distance and a change of 37° in the α_3 angle, a progression of 20−40 coupled vibrations must occur to account for the magnitude of the

(31) Brint, P. Private communication.
(32) Bersuker, I. B. *Coord. Chem. Rev.* **1975**, *14*, 357.
(33) Bersuker, I. B. *The Jahn-Teller Effect and Vibronic Interactions in Modern Chemistry*; Plenum Press: New York, 1983.

observed changes. Such a progression can be considered as a plot of the structural pathway from the +A route to the −A route of Figure 6, involving the coupled $\nu_{sym}^{str} + \nu_{sym}^{bend}$ modes of vibration, with the six data points representing six individual structures along the structural pathway, with each data point characterized by a full single crystal X-ray structure determination. Two further data points are involved along the central correlation of Figure 4c if the phen/Cl data points are included.

In order to explain the occurrence of the parallel correlations in Figure 4c, *n* modes of a *single* vibration, $\pm\nu$, where $n = 8-10$, must be involved in order that the parallel displacement can be observed, Figure 6, points **II** and **III**. This is then followed by a progression of the coupled modes (in order that a linear correlation can be observed) separate but parallel to the central linear correlation. This observation of parallel linear correlations in the same plot, Figure 4c, requires the addition of both the Cl^- and I^- data points but is then one of the best pieces of evidence for both structural pathways and parallel pathways and originates from the amplification factor[32] in the *pseudo*-Jahn-Teller effect.[33]

The various plots also suggest that the directions of distortion from RTB to RSBP could be associated with the modes of vibration of the CuN_4Br chromophore, Figure 5. The ±A route is restricted to the ν_{sym}^{str} and ν_{sym}^{bend} modes of vibration and the ±B route distortions with the ν_{asym}^{str} and ν_{asym}^{bend} modes of vibration. However, as the actual data points rarely involve pure % A or % B contributions, Table 6, all four modes are generally involved in the distortion of each complex, unless a 2-fold axis of symmetry is involved. Even with the six linear Br^- data points of Figure 4c, each is accompanied by some +B route distortion, Table 6.

Implications. The four scatter plots of the [Cu(phen)$_2$X]-[Y] data points, X = Cl^-, Br^-, and I^- clearly suggest that the distribution with respect to the RTB and RSBP data points is not random, but consistent with linear and parallel structural pathways, in which the effect of vibronic coupling[33] is seen *directly* in the scatter plots of Figure 4. If so, the [Cu(phen)$_2$X]-[Y] data represent the best evidence for the involvement of vibronic coupling to account for the structural consequences of the plasticity effect[34] in the series of cation distortion isomers[18,19] of the copper(II) ion. Of equal importance is the wide range of stereochemistry displayed by the *same* $[Cu(phen)_2Br]^+$ cation, from near RTB, $\tau = 0.95$, to TBDSBP, $\tau = 0.22$. In the past, a number of accounts have been given[35−37] to describe the static geometries of the five coordinate stereochemistries of *different* ML_5 chromophores and try to account for these changes in terms of the different bonding roles of the ligands present.[36] The present paper emphasizes that, in the special case of the low-symmetry CuN_4X chromophore, vibronic coupling associated with the *pseudo*-Jahn−Teller effect[33] can also produce the *same* range in stereochemistry of the five coordinate ML_5 chromophore with the *same* set of ligands. Small differences in the crystal field effects of the different counteranions, balancing the vibronic coupling effects, result in the observed small differences in the observed structures of the cations. The present script suggests a dynamic involvement of a number of the modes of vibration of the central chromophore to produce the changes

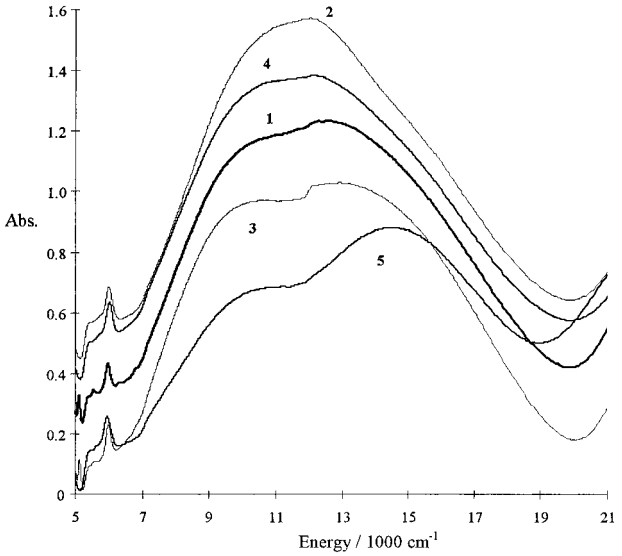

Figure 8. Electronic reflectance spectra of some [Cu(phen)$_2$Br][Y] complexes.

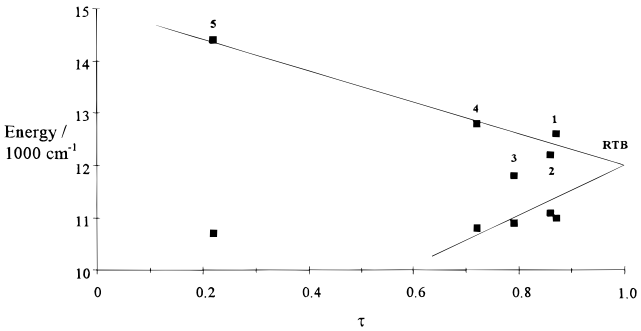

Figure 9. Electronic criterion of stereochemistry illustrated by correlating the peak energy and appearance with the change in stereochemistry from RTB to RSBP.

associated with the movements about the potential energy surface of the structural pathway in which individual points are characterized by single crystal X-ray structure determinations of the same cation distortion isomers.[18,19]

Electronic Properties of the [Cu(phen)$_2$Br][Y] Complexes. The polycrystalline electronic reflectance spectra of **1**−**5** are shown in Figure 8. For **1**, **2**, and **4**, a broad asymmetric peak occurs at 12 600, 12 000, and 11 800 cm^{-1}, respectively, with some evidence for a possible low-energy shoulder at 11 000, 11 100, and 10 900 cm^{-1}, respectively, consistent with near TB stereochemistries ($\tau = 0.87-0.72$). The spectrum of **3**, $\tau = 0.79$, shows a broad peak beginning to split into two. These two peaks involve energies of 10 800 and 12 800 cm^{-1} and appear to evolve from the single peak at 12 000 cm^{-1} for a RTB stereochemistry. The suggested one-electron ground state configuration[20,38] is $d_{z^2} > d_{xy} \approx d_{x^2-y^2} > d_{xz} \approx d_{yz}$. The principal absorption may be assigned as a $d_{xz} \approx d_{yz} \rightarrow d_{z^2}$ transition, with the low-energy shoulder assigned as a $d_{x^2-y^2} \rightarrow d_{z^2}$ transition.

Complex **5**, $\tau = 0.22$, which has a TBDSBP stereochemistry, involves a high-energy peak at 14 400 cm^{-1}, with a low-energy shoulder at lower intensity at 10 700 cm^{-1}. The suggested one-electron ground state configuration is $d_{x^2-y^2} > d_{z^2} > d_{xy} > d_{xz} \approx d_{yz}$. The transitions may be assigned as the $d_{z^2} \rightarrow d_{x^2-y^2}$ transition for the low-energy peak and the $d_{xz} \approx d_{yz} \rightarrow d_{x^2-y^2}$ transition for the high-energy peak.

The change in peak energy and intensity for the series of six [Cu(phen)$_2$Br][Y] complexes can be used to establish an

(34) Gazo, J.; Bersuker, I. B.; Garaj, J.; Kabesova, M.; Kohout, J.; Langfelderova, H.; Melnik, M.; Serator, M.; Valach, F. *Coord. Chem. Rev.* **1976**, *21*, 253.
(35) Muetterties, E. L.; Guggenberger, L. T. *J. Am. Chem. Soc.* **1974**, *96*, 1748.
(36) Holmes, R. R.; Deiters, J. A. *J. Am. Chem. Soc.* **1977**, *99*, 3318.
(37) Auf der Heyde, T. P. E.; Burgi, H.-B. *J. Am. Chem. Soc.* **1989**, *28*, 3960, 3970, 3982.
(38) Hathaway, B. J. *J. Chem. Soc., Dalton Trans.* **1972**, 1192.

electronic criterion of stereochemistry,[38] Figure 9. RTB stereochemistry shows a single peak at ~12 000 cm^{-1}, SBPDTB stereochemistry shows two clearly resolved peaks at ~11 000 and ~13 000 cm^{-1}, with near SBP stereochemistry showing a high-energy peak at ~14 500 cm^{-1} and a low-energy shoulder at ~11 000 cm^{-1}.

Acknowledgment. The authors acknowledge the award of Forbairt and University College Cork (UCC) Studentships (to G.M., C.O.'S. and B.M.), an EOLAS grant for the diffractometer, the Computer Bureau, UCC for computing facilities, Professor G. M. Sheldrick and Drs. P. Roberts, S. Motherwell, K. Henrick, A. L. Spek, and P. McCardle, for the use of their programs, and the Microanalysis Section, UCC, for analysis.

Supporting Information Available: Tables of fractional atomic coordinates (Table S1), fractional atomic coordinates for the hydrogen atoms (Table S2), anisotropic thermal parameters (Table S3), complete bond distances (Table S4), complete bond angles (Table S5), and selected mean plane data (Table S6) for complexes **1**−**5** (38 pages). Ordering information is given on any current masthead page.

IC970458A